JOURNAL OF GEOPHYSICAL RESEARCH, VOL. 102, NO. B2, PAGES 2807–2814, FEBRUARY 10, 1997

A comparison of geoid undulations for west central Greenland

Daniel R. Roman,[1] Beata Csathó,[1] Kenneth C. Jezek,[1] Robert H. Thomas,[2] William B. Krabill, [3] Ralph R. B. von Frese, [4] and Rene Forsberg [5]

Abstract. The accuracy of a new local gravity field model, GEOID94A, is examined at a site on the western Greenland ice sheet. The model, developed by the Danish National Survey and Cadastre, incorporates several new gravity data sets including an extensive amount of airborne gravity data. Model-derived geoid undulations were compared to independently determined undulations found by differencing the elevations from Global Positioning System controlled airborne laser altimetry and optical leveling surveys. Differences between the two sets of undulations were less than +/-6 cm RMS. The comparison improved (+/-5 cm RMS) when GEOID94A undulations were adjusted by local gravity observations also acquired at the site. Our comparisons demonstrate that GEOID94A adequately models the long to intermediate wavelengths of the gravity field. We conclude that GEOID94A constitutes a reliable reference model for studies of Greenland's gravity field.

Introduction

Gravity field models provide a reference for interpreting local and regional gravity data. However, current global models (OSU91A, JGM2, etc.) are derived based on only limited observations for remote regions [*Rapp et al.*, 1991; *Nerem et al.*, 1994]. Hence the reliability and utility of these models are reduced for those regions. A new model, the Danish GEOID94A [*Forsberg*, 1994], incorporates data from an airborne gravity survey over most of interior Greenland. The inclusion of this new data warrants a closer examination of the model.

To evaluate GEOID94A, a comparison was made with a profile of independently determined geoid undulation differences measured along a 42 km survey line located on the western flank of the Greenland ice sheet (Figure 1). Figure 1 shows a main NE-SW trending profile with two crossing profiles. Only the NE-SW profile is examined here. The independent undulations were derived from the topographic difference of airborne laser altimetry and optical leveling survey measurements. The laser system measured the height of the ice surface above the ellipsoid (ellipsoidal height). The leveling surveys measured the relative height change above the geoid (relative orthometric height). The difference of the two heights was the relative geoid undulation [e.g., *Heiskanen and Moritz*, 1967; *Rapp and Pavlis*, 1990].

Relative gravity observations were made at about 1 km intervals along the 42 km line. These measurements were combined with GEOID94A values through a point mass inversion technique [*von Frese et al.*, 1981] to obtain better estimates of local geoid undulations. These adjusted undulations were then compared with the laser/leveling- derived undulations.

Airborne Oceanographic Lidar (AOL) System

Airborne laser altimetry is particularly suited for fast and precise elevation measurements in remote areas. It can provide submeter accuracy by using Global Positioning System (GPS) and inertial navigation system (INS) measurements to determine aircraft position and attitude. Laser profiling systems have only one laser element pointing at nadir and a single range measurement is performed for each laser pulse. Laser scanning systems contain movable optics or multiple laser elements. These are superior when aerial coverage, precise overflight of known surface points, or repeat flights (mapping surface changes) are needed.

NASA has developed several different airborne and spaceborne laser systems over the years. The airborne oceanographic lidar (AOL) system was originally designed and developed for shallow water bathymetry, but it has been successfully used for various applications on land (Krabill et al., 1984; Krabill and Swift, 1987) and

[1] Byrd Polar Research Center, Ohio State University, Columbus.

[2] NASA Headquarters, Washington, D.C.

[3] Observational Science Branch, Laboratory for Hydrospheric Processes, Goddard Space Flight Center/Wallops Flight Facility, NASA, Wallops Island, Virginia.

[4] Geological Sciences Department, Ohio State University, Columbus.

[5] National Survey and Cadastre, Geodetic Division, Copenhagen, Denmark.

Paper number 96JB02697.
0148-0227/97/96JB-02697$09.00

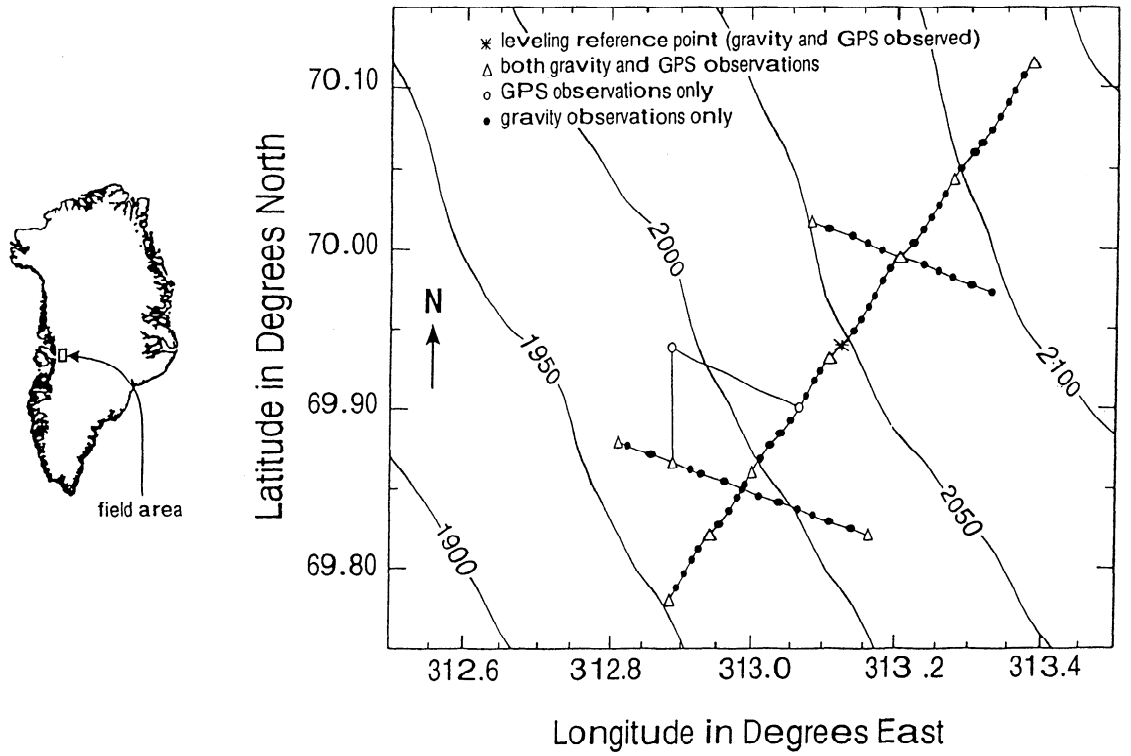

Figure 1. Location of the Greenland field area with ellipsoid elevation contours (in meters) of the ice sheet surface shown. Solid circles denote stations where gravity observations were obtained. Open circles denote stations where surface Global Positioning System (GPS) observations were made. Triangles denote stations where both are obtained. All stations were optically leveled using station N10 for reference (denoted by the asterisk).

on ice sheets. The latter includes detection of ice sheet elevation changes [*Krabill et al.*, 1995b; *Thomas et al.*, 1993, 1995] and mapping ice sheet features, such as surface undulations and lakes [*Csathó et al.*, 1995, 1996].

The laser scanning system of the AOL system covers a 130-200 m wide swath on the ground within a set of overlapping spirals (Figure 2). The transmitter is a pulsed laser that operates in the visible part of the spectrum. The laser beam is directed along an oval shaped pattern with the help of a nutating mirror. In 1991, the aircraft flew 400 m above the ground yielding a laser spot on the ground approximately 0.6 m in diameter. With a laser pulse of 800 Hz and with five conical scans per second, the maximum along track separation was less than 4 m. In order to provide higher data density, the laser pulse was gradually increased. In 1993, the system used a pulse rate of 2000 Hz with five conical scans per second.

The system was mounted on a P-3 aircraft [*Krabill et al.*, 1995a]. The aircraft location was determined with the kinematic GPS technique of tracking the difference in the GPS dual frequency carrier-phase-derived ranges from a fixed receiver located over a precisely known benchmark and a mobile receiver on the aircraft [*Krabill and Martin*, 1987]. The attitude information was obtained from an inertial navigation system (INS). Real-time GPS data were used to provide the pilot with a visual display of the flight line and the current offset from the desired track.

Although many factors affected the accuracy of the measurements, the principal sources of the point error were the laser ranging error and the position and attitude errors from the GPS and INS. Numerous tests were performed by NASA including internal and in-flight calibration, comparison of neighboring points, and crossing and repeat flights. The results indicated that ice-surface elevations could be reliably measured by the AOL system to a +/-20 cm root mean square (RMS) over baselines of more than 700 km [*Krabill et al.*, 1995a].

Data

Relative surface gravity observations, spot GPS measurements, snow accumulation data, AOL surface elevation, and leveling data were gathered in the field area (Figure 1). Field gravity observations were obtained with a LaCoste-Romberg gravimeter. Drift and tares were detected based on repeated measurements at the base camp. After all adjustments, the standard errors of the relative gravity values for repeated stations were +/-0.1 mGal. There were four stations that had higher differences (no greater than +/-0.3 mGal) between repeat visits located 10 km south of station N10. The source of these residual differences was probably an incomplete tare removal. The relative gravity measurements were converted to absolute gravity using six control stations of known absolute gravity in Sondre Stromfjord and Jakobshavn, Greenland. The accu-

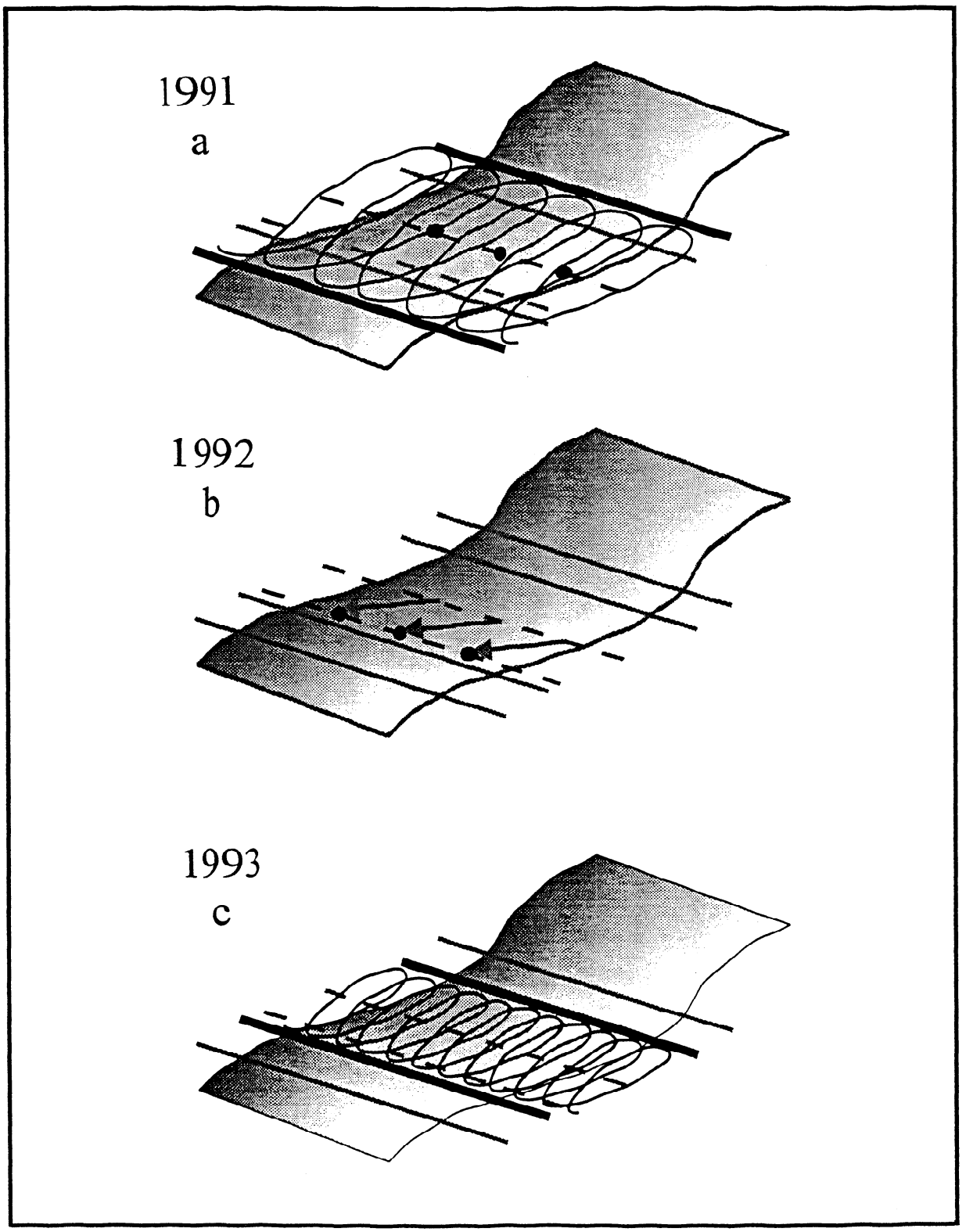

Figure 2. Physical relationships between leveling and airborne oceanographic lidar (AOL) observations are shown. Data gathered in the 3 listed years (bold features) are spatially compared to data from other years (gray features). AOL ground swaths are shown as swirls with the extents shown as solid lines. Leveling lines are shown as dashed lines with dots for stations. (a) Surface leveling stations and circular AOL ground swath for 1991. Note that both 1991 (bold dashed line) and 1992 (gray dashed line) are contained in the AOL ground swath. (b) Joint gravity/leveling stations for 1992. Oblique arrows show the movement of the stations from 1991 (gravy dashed line) to 1992 (bold dashed line). (c) AOL ground swath for 1993 (narrower than that of 1991) containing the locations of the 1991 and 1992 leveling lines (both shown as gray dashed lines).

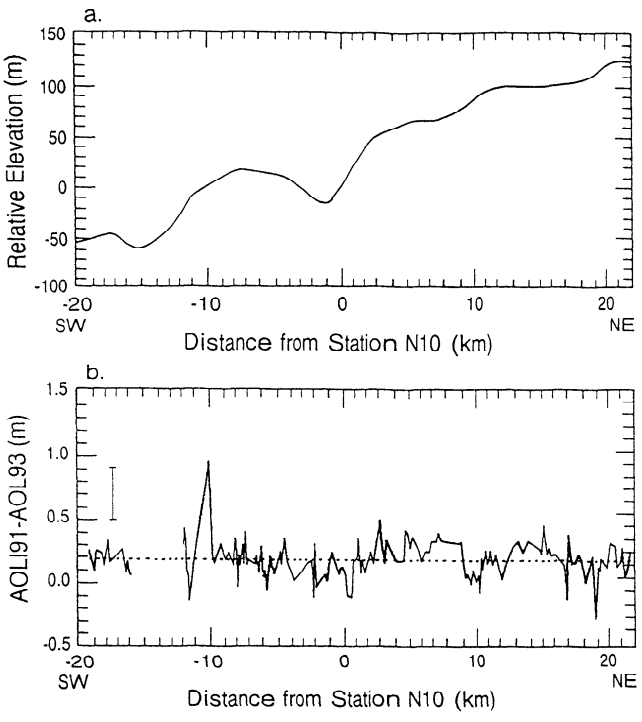

Figure 3. (a) Surface topography from 1991 leveling. (b) Change of the ice sheet surface between 1991 and 1993 derived by differencing AOL measurements (solid line). A first-order fit (dashed line) is also shown. An estimate of the standard error is shown by the bar on the left.

racy of these International Gravity Standardization Net (IGSN) sites is an order of magnitude smaller than that of the field stations.

Spot GPS measurements were obtained on the surface using a geodetic receiver simultaneous to the leveling surveys. There were two GPS stations in 1991 and 15 in 1992 [*Sohn et al.*, 1994]. GPS solutions for ellipsoidal height had standard errors of between +/-20 cm. The GPS measurements provided an absolute ellipsoidal coordinate reference frame for all surface measurements.

AOL surface elevation data were collected during 3 consecutive days in September 1991 (four flights) and in 1 day in July 1993 (two flights). In 1991, AOL surface elevations were collected in a broad swath that enveloped the surface locations where leveling and GPS data were gathered (Figure 2a). All gravity, leveling, and GPS data gathered at the 1992 locations fell within the ground swath of the 1991 AOL observations (Figure 2b). Note that the movement of the ice (about 90 m/year) was oblique to the central axis of the field area stations. In 1993, further AOL elevation data were gathered in a swath that also covered the 1991 and 1992 locations of the field area (Figure 2c). The ellipsoidal heights for the profile were computed by averaging all the AOL observations in a neighborhood of 10 by 10 m. Because of the dense coverage provided by the AOL, usually there was at least one AOL point (more often 2-6) in this neighborhood.

Krabill et al., [1995a] analyzed these AOL data sets to assess random and systematic errors. RMS differences

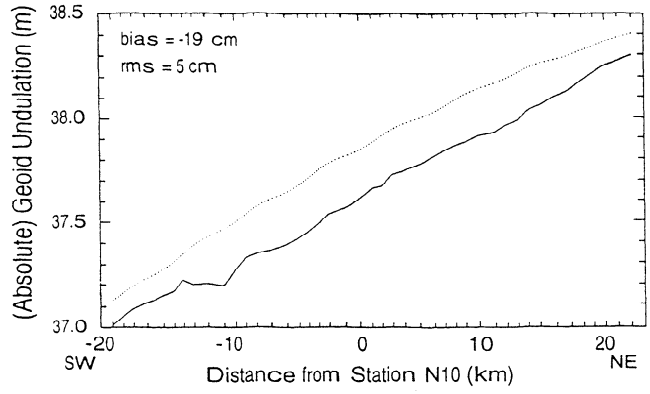

Figure 4. Geoid undulations determined from observed gravity and the GEOID94A model are shown as a solid line. Undulations determined only from the GEOID94A model are shown as a dotted line. The -19 cm bias and +/-5 cm RMS difference demonstrate the effects of incorporating the gravity data.

occurring over short segments of the flight path were estimated at +/-15 cm. During periods of poor GPS satellite coverage (4-5 satellites), biases between tracks up to 20 cm were detected. During periods of good GPS coverage (6-7 satellites), biases were reduced to the 10 cm level. GPS coverage was typically poor in 1991 and improved in 1993.

Optical leveling data were acquired in 1991 and 1992 [*Sohn et al.*, 1994] to determine the relative orthometric heights for the profile. The average station spacing for the leveling surveys was about 135 m along the 42 km long NE-SW axis [*Sohn et al.*, 1994]. Leveling data were referenced to station N10, located in the middle of the field area (Figure 1). An open-loop leveling survey was conducted in 1991; a closed-loop survey was conducted in 1992 with 5.2 cm closure error for a 30 km loop. Acquisition of the 1991 leveling data was made under adverse weather conditions and may be less reliable. The resulting relative orthometric elevation profile for 1991 is shown in Figure 3a. The profile for 1992 was similar.

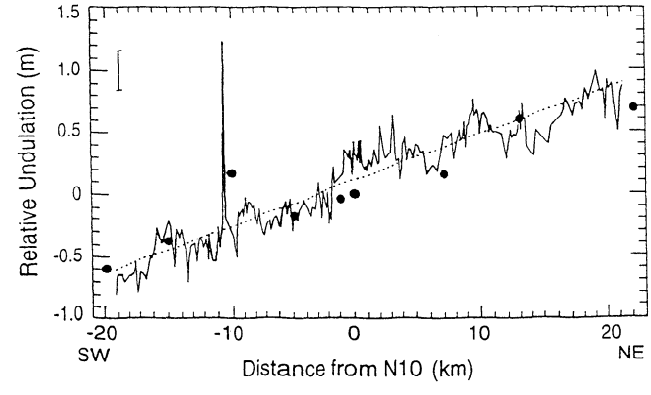

Figure 5. Topographic geoid undulations derived from AOL and optical leveling survey (optical leveling, August 1991 and AOL, September 18, 1991) are shown (solid line). A first-order fit (dotted line) and the geoid undulations derived from surface GPS measurements (solid circles) are also shown. An estimate of the standard error is shown by the bar on the left.

Table 1. Bias, RMS of the Fit, Slope, and Total Height Differences (Δh) Over the 42 km Leg for the First-Order Estimates of the Topographic Geoid Undulation.

AOL mission		1992 level line				1991 level line			
Date	Direction	Bias, m	RMS, m	Slope, m/km	Δh, m	Bias, m	RMS, m	Slope, m/km	Δh, m
September 18, 1991	N → S	0.112	0.175	0.037	1.554	-0.059	0.129	0.037	1.554
September 19, 1991	N → S	-0.111	0.144	0.035	1.470	-0.291	0.139	0.036	1.512
September 20, 1991	N → S	0.304	0.156	0.033	1.386	0.122	0.133	0.034	1.428
September 20, 1991	S → N	0.153	0.125	0.034	1.428	-0.040	0.121	0.035	1.470
June 6, 1993	S → N	0.040	0.132	0.031	1.302	-0.230	0.095	0.031	1.302
July 9, 1993	S → N	0.011	0.136	0.032	1.344	-0.167	0.108	0.032	1.344

Average Slope is 0.0339 m/km; Standard Deviation is 0.00215 m/km.

Glaciologic Setting

As shown in Figure 3a, the study area was characterized by rounded hills and valleys with wavelengths of about 10 km and surface undulations of about 50 m. Snow accumulation was about 1.2 m/y [*Sohn et al.*, 1994], and accumulated amounts were spatially modulated by the topography. Figure 3b shows changes in surface topography over a 2 year period. The generally constant shape indicates snow accumulation and drift patterns were nearly constant over time. The high-frequency variability (+/-15 cm) was apparently due to randomly distributed snow dunes (sastrugi), which had an amplitude of about 5 cm, and by local variability in snow accumulation. There is a 15 cm bias in the data that we attributed to instrumental effects rather than a real height change of the glacier surface. The peak in Figure 3b, around -10 km, was due to snow drifts that had accumulated around the NASA camp.

The GEOID94A Model

GEOID94A is a regional geoid undulation field model for Greenland that was generated by the Danish National Survey and Cadastre (KMS). Using the OSU91A model for a priori values, it has been computed on a 5 x 5 arcminute grid by spherical Fast Fourier Transform (FFT) methods [*Forsberg and Sideris*, 1993] and incorporates many coastal, shipborne, satellite, and airborne measurements not included in any other model. Danish coastal surveys, both onshore and on the ice, as well as shipborne measurements provide excellent coverage of the coastal regions of Greenland. This is further complimented by the utilization of digital terrain models of surface topography and ice thickness from radar soundings. However, the incorporation of airborne gravity measurements at about a 30 km track spacing throughout the interior introduces the most significant change over previous Danish models [*Forsberg*, 1993, 1994]. No formal error assessments are currently available for this model. An associated 5 arcminute grid model also provides gravity anomalies based on the same measurements and analysis.

Adjustment of GEOID94A Undulations

Geoid undulations and gravity anomalies were determined from the GEOID94A models by interpolating the 5 arcminute grid values to the observation station locations. The interpolated undulations were then adjusted using a point mass inversion to incorporate the corrected gravity observations. Calculated gravity values based upon GEOID94A gravity anomalies were differenced with the corrected gravity observations. These residuals were then used to adjust the original GEOID94A undulations.

The original GEOID94A and the gravity-adjusted GEOID94A undulations are shown in Figure 4. There is a 19 cm bias between the two profiles with an RMS difference of +/-5 cm. The bias and the presence of 1 km wavelength features in the adjusted undulations

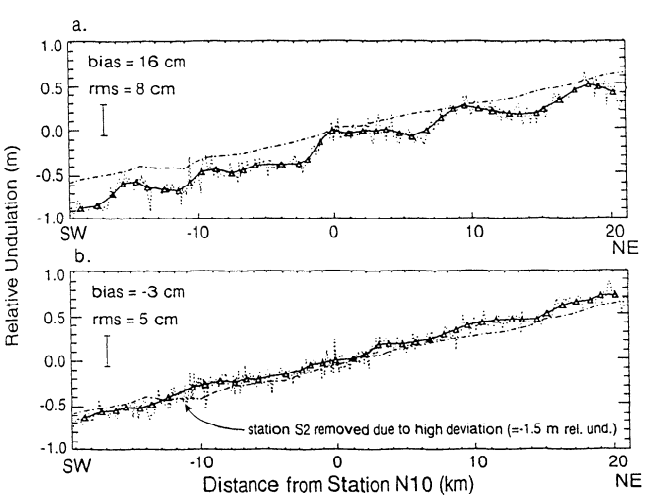

Figure 6. Topographic geoid undulations for the 1991 and 1992 level lines obtained by averaging all differences with AOL observations (dotted line). Their smoothed and thinned versions are used for further comparison (solid line). Locations of the gravity stations are depicted with triangles. The gravity adjusted GEOID94A undulations are also overplotted (dashed-dotted line). An estimate of the standard error is shown by the bar on the left. (A) The 1991 level line. (b) The 1992 level line.

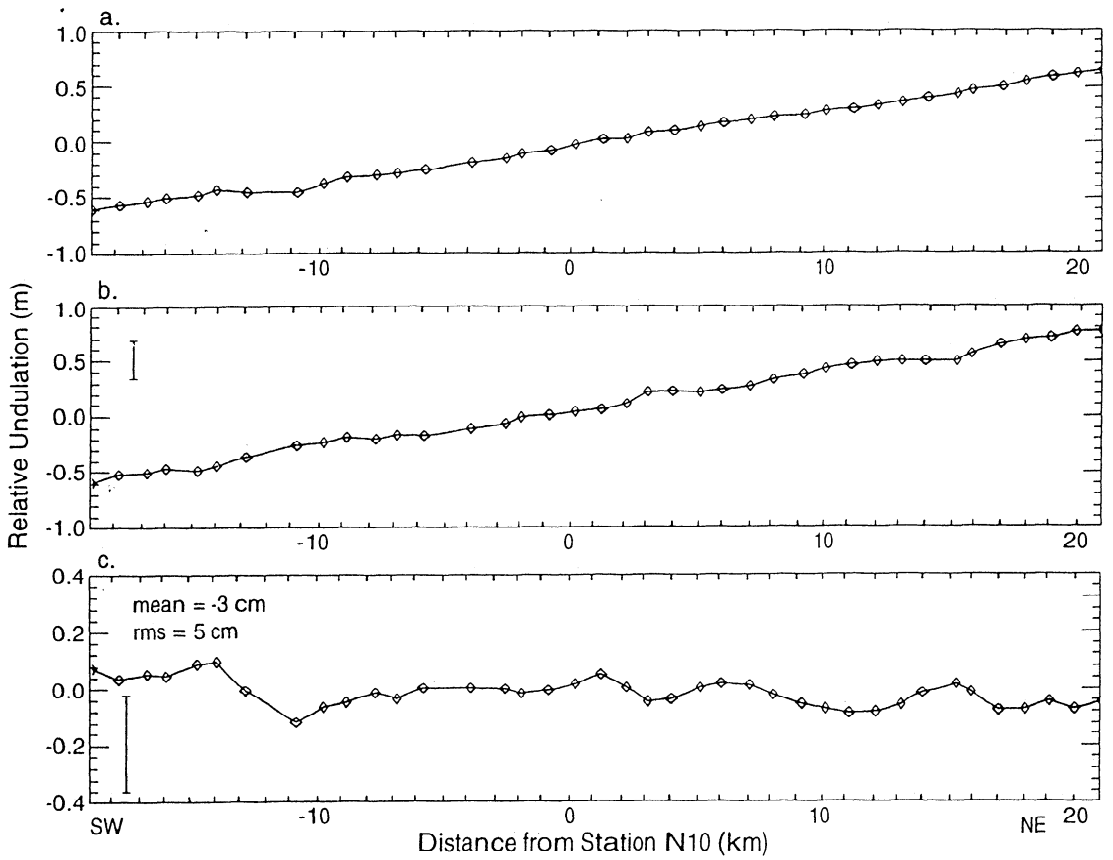

Figure 7. (a) The gravity-adjusted GEOID94A undulations in which no errors were assigned, and (b) the smoothed AOL/leveling-derived geoid undulations. An estimate of the standard error is shown by the bar on the left. Gravity station locations are shown as diamonds. (c) Differences of Figures 7a. and 7b. above. An estimate of the standard error is shown by the bar on the left.

resulted from the incorporation of the gravity measurements. The height change over the 42 km profile for both the original and adjusted undulations was 1.28 m, which resulted in the same slope (0.030 m/km). The original model-derived undulation for station N10 was 37.85 m, and the adjusted undulation was 37.61 m. These values were removed from the respective profiles to generate relative undulations that reference the same station as the leveling data. The +/-0.1 mGal RMS error for the gravity observations affected the adjusted undulations to less than the centimeter level. As no error assessment is available for the original undulations and the effects of the gravity data are subcentimeter, no errors were assigned in the adjusted undulations.

Undulations Derived From Laser Altimetry and Leveling

Relative geoid undulations were estimated by differencing coincident ellipsoidal and orthometric heights. No absolute geoid undulations could be determined from our topographic data, because the orthometric heights were referenced to an arbitrary point (N10). Undulations were computed for both leveling lines using the six AOL flights (12 combinations). As an example, the one computed using the September 18, 1991, AOL flight along the 1991 leveling line is shown in Figure 5.

Also shown are estimates of the geoid undulations derived by differencing the simultaneously acquired surface GPS measurements (positions noted in Figure 1) and optical leveling data sets [*Sohn et al.*, 1994]. The good agreement between the AOL- and GPS-derived undulations suggested that there were minimal time dependent processes, such as variable snow accumulation, affecting the study.

Lines were fit to the AOL/leveling-derived geoid undulations (Table 1). The slope of the fitted line, its bias relative to N10, the RMS of the fit, and the total height difference over the 42 km section have been computed for the different AOL/leveling combinations. The slope of the fitted lines approximated the slope of the local geoid undulations. The RMS error of the fit was due to errors in AOL and leveling heights. The causes of the large (20 cm) differences in biases between AOL elevation profiles were discussed above.

We estimated the AOL/leveling-derived geoid undulations in the following fashion. The biases calculated in Table 1 were removed from the data and then all the 1991 and 1992 observations are averaged. The random noise is reduced by using a 13-term moving average

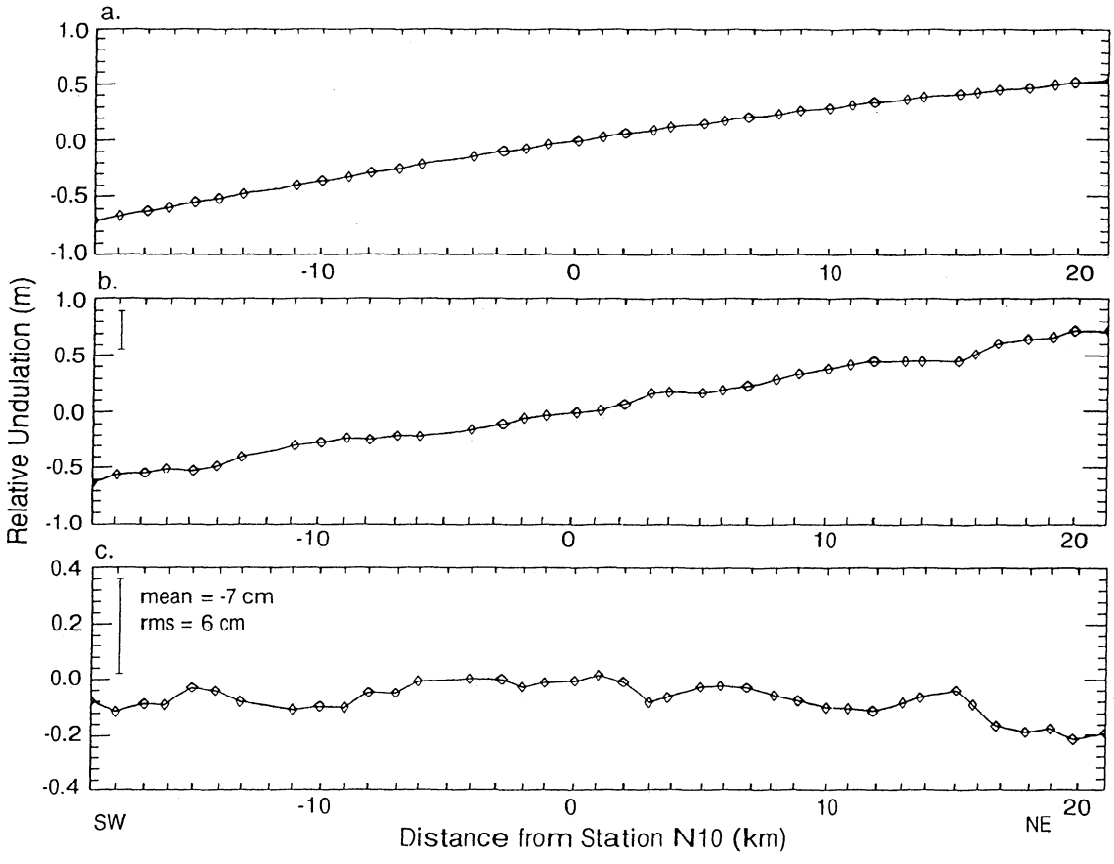

Figure 8. (a) The GEOID94A model undulations (without gravity observations) in which no errors were assigned, and (b) the smoothed AOL/leveling-derived geoid undulations. An estimate of the standard error is shown by the bar on the left. Gravity station locations are shown as diamonds. (c) Differences of 8a. and 8b. above. An estimate of the standard error is shown by the bar on the left.

filter, and the data set is thinned by calculating the undulations only at the gravity station positions.

In Figures 6a and 6b, the relative undulations are plotted using the averaged AOL data and the 1991 and 1992 leveling data, respectively. The smoothed AOL/leveling-derived undulations are shown with the thick line. For reference, the original (unsmoothed) AOL/leveling-derived undulations are overplotted in a dotted line. The individual gravity stations are shown as triangles. The gravity-adjusted GEOID94A derived undulations are plotted as a dashed-dotted line for comparison. The RMS difference was +/-5 cm between the gravity-adjusted GEOID94A undulations and the 1992 AOL/leveling-derived undulations. The RMS difference for the 1991 data set comparison was +/-8 cm. Biases between the adjusted GEOID94A-derived undulations and the AOL/leveling-derived undulations were caused by the selection of N10 as an arbitrary reference height point. Consequently, biases should be ignored.

The 1991 AOL/leveling-derived undulations included a 10 km wavelength feature with a 15 cm amplitude (Figure 6a). This wavelength corresponds to the glacier surface topography. It is not observed in the 1992 undulations. We attributed this feature to operator errors that occurred during the more difficult 1991 measurements season. Subsequent discussion will focus on the 1992 data set.

Comparisons

Gravity-adjusted GEOID94A undulations (Figure 7a) are compared to the 1992 AOL/leveling-derived undulations (Figure 7b). The residuals are shown in Figure 7c. The slopes of the two geoid undulation profiles are similar (Figures 7a and 7b). The height difference between the ends of the residual profile is about 10 cm (Figure 7c). The relatively large 20 cm signal approximately 10 km south of station N10 (to the left in Figure 7c) is located near the stations that had incompletely removed tares. The RMS difference between the gravity-adjusted GEOID94A undulations and the 1992 AOL/leveling-derived undulations is +/-5 cm.

The differences between the GEOID94A model undulations uncorrected for observed gravity (Figure 8a) and the 1992 AOL/leveling-derived undulations (Figure 8b) are shown in Figure 8c. Many of the high-frequency features observed in the residuals in Figure 7c are seen in Figure 8c. We attributed the 10 km wavelength

features in Figures 7c and 8c to leveling uncertainties and stochastic changes in snow accumulation patterns weakly coupled with surface topography. These 10 km features were similar to those observed in the 1991 leveling data (Figure 6a) but not of the same amplitude.

The height difference between the ends of the residual profile is about 20 cm (Figure 8c). A distinct slope from the southern to the northern ends of the profile (left to right in Figure 8c) is more clearly visible than in Figure 7c. The RMS difference between the GEOID94A model undulations (without gravity observations) and the 1992 AOL/leveling-derived undulations is +/-6 cm.

Conclusions

Our comparisons show that the GEOID94A model approximates the gravity field in our study area for intermediate and long wavelengths (+/-6 cm RMS differences). By using additional local gravity data to adjust GEOID94A, we observe a better comparison because a small slope and bias in the modeled field is removed (+/-5 cm RMS differences). We conclude that the GEOID94A undulations adequately approximate the gravity field in intermediate and long wavelengths. Inclusion of our local gravity data appears to correct a shorter wavelength term, resulting in a small improvement in the predicted undulations.

The gravity data discussed in this study were collected as part of a much larger and ongoing NASA project that has now acquired surface topography and surface gravity data around the entire Greenland Ice Sheet. The small, centimeter scale differences detected in our comparison between modeled and measured undulations indicate that GEOID94A will provide a satisfactory reference model for incorporating these new data in studies of Greenland's subglacial crust.

Acknowledgments. This work has been supported by NASA's Polar Ocean and Ice Sheet Program.

References

Csathó, B., T.F. Schenk, R.H. Thomas, and W.B. Krabill, Topographic mapping by laser altimetry, in *Proceedings of SPIE, Remote Sensing and Reconstruction for Three-Dimensional Objects and Scenes*, vol. 2572, edited T.F. Schenk, pp. 10-20, SPIE Opt. Eng. Press, Bellingham, Wash., 1995.

Csathó, B., R.H. Thomas, and W.B. Krabill, Mapping ice sheet topography with laser altimetry in Greenland, it BPRC Tech. Rep. 96-01, Byrd Polar Res. Cent., Ohio State Univ., Columbus, 53 pp., 1996.

Forsberg, R., Impact of airborne gravimetry on geoid determination - The Greenland example, *Bull. 2*, 32-43, Int. Geoid Serv., D.I.I.R., Politecnico di Milano, Italy, 1993.

Forsberg, R., Gravity and GPS in Greenland, paper presented at General Assembly, Nordic Geod. Comm., Ullensvang, Norway, May 1994.

Forsberg, R., and M.G. Sideris, Geoid computation by the multiband spherical FFT approach, *Bull. Manuscr. Geod. 18*, 82-90, 1993.

Heiskanen, W.A., and H. Moritz, *Physical Geodesy*, W.H. Freeman, New York, 364 pp., 1967.

Krabill, W.B., and C.F. Martin, Aircraft positioning using global positioning carrier phase data, *J. Inst. Navig., 34*, 1-21, 1987.

Krabill, W.B., and R.N. Swift, Airborne lidar experiments at the Savannah River plant, *NASA Tech. Memo. 4007/DOE/SR/14075-1*, 1987.

Krabill, W.B., J.G. Collins, L.E. Link, R.N. Swift, and M.L Butler, Airborne laser topographic mapping results, *Photogramm. Eng. Remote Sens., 50* (6), 685-694, 1984.

Krabill, W.B., R.H. Thomas, C.F. Martin, R.N. Swift, and E.B. Frederick, Accuracy of airborne laser altimetry over the Greenland ice sheet, *Int. J. Remote Sens., 16* (7), 1211-1222, 1995a.

Krabill, W. B., R. H. Thomas, K. Jezek, K. Kuivinen, and S. Manizade, Greenland ice sheet thickness changes measured by laser altimetry, *Geophys. Res. Lett., 22* (17), 2341-2344, 1995b.

Nerem, R.S., et al., Gravity model development for TOPEX/POSEIDON: Joint gravity models 1 and 2, *99*(12), 24421-24447, 1994.

Rapp, R.H., and N.K. Pavlis, The development and analysis of geopotential coefficient models to spherical harmonic degree 360, *J. Geophys. Res., 95* (13), 21885-21911, 1990.

Rapp, R.H., Y.M. Wang, and N.K. Pavlis, The Ohio State 1991 geopotential and sea surface topography harmonic coefficient models, *Dep. of Geod. Sci. and Surv. Rep. 410*, Ohio State Univ., Columbus, 94 pp., 1991.

Sohn, H.-G., K.C. Jezek, R.H. Thomas, K. Kuivinen, and B. Csathó, Greenland ice sheet mapping with optical leveling and global positioning system, *BPRC Tech. Rep. 94-03*, Byrd Polar Res. Cent., Ohio State Univ., Columbus, 98 pp., 1994.

Thomas, R.H., W.B. Krabill, S. Manizade, R. Swift, and A. Brenner, Comparison of radar-altimetry data over Greenland with surface topography derived from airborne laser altimetry, paper presented at Second ERS-1 Symposium - Space at the Service of our Environment, ESA, Hamburg, Germany, October 11-14, 1993.

Thomas, R.H., W.B. Krabill, E. Frederick, and K. Jezek, Thickening of Jakobshavns Isbræ, West Greenland, measured by airborne laser altimetry, *Ann. Glaciol., 21*, 259-262, 1995.

von Frese, R. R. B., W. J. Hinze, and L. N. Braile, Spherical Earth gravity and magnetic anomaly analysis by equivalent point source inversion, *Earth Planet. Sci. Lett., 53*, 69-83, 1981.

B. Csathó, K.C. Jezek, and D.R. Roman, Byrd Polar Research Center, Ohio State University, 108 Scott Hall, 1090 Carmack Rd., Columbus, OH 43210-1002. (e-mail: csatho@ohglas.mps.ohio-state.edu; jezek@iceberg.mps.ohio-state.edu; roman@iceberg.mps.ohio-state.edu)

R. Forsberg, KMS (National Survey and Cadastre), Geodetic Division, Rentemestervej 8, DK-2400 Copenhagen NV, Denmark. (e-mail: rf@kms.min.dk)

W.B. Krabill, Code 972, Observational Science Branch, Laboratory for Hydrospheric Processes, GSFC/Wallops Flight Facility, NASA, Building N-159, Wallops Island, VA 23337. (e-mail: krabill@osb.wff.nasa.gov)

R.H. Thomas, Code YS, NASA Headquarters, 300 E St. SW, Washington, DC 20546. (e-mail: rthomas@hq.nasa.gov)

R.R.B. von Frese, Department of Geological Sciences, Ohio State University, 376 Mendenhall Lab, 125 South Oval Mall, Columbus, OH 43210-1398. (e-mail: vonfrese@geology.ohio-state.edu)

(Received November 17, 1995; revised August 28, 1996; accepted September 3, 1996.)